


 Cite this: *RSC Adv.*, 2022, 12, 19741

# Ionic liquid-immobilized silica gel as a new sorbent for solid-phase extraction of heavy metal ions in water samples†

 The Thai Nguyen,<sup>ab</sup> Tu-Hoai Duy Nguyen,<sup>ab</sup> Tam Thanh Thi Huynh,<sup>ab</sup> Minh-Huy Dinh Dang,<sup>bc</sup> Linh Ho Thuy Nguyen,<sup>bc</sup> Tan Le Hoang Doan,<sup>bc</sup> Thinh Phuc Nguyen,<sup>bd</sup> Mai Anh Nguyen<sup>\*bd</sup> and Phuong Hoang Tran<sup>id\*ab</sup>

In the current study, we have developed a solid-phase extraction (SPE) method with novel C18-alkylimidazolium ionic liquid immobilized silica (SiO<sub>2</sub>-(CH<sub>2</sub>)<sub>3</sub>-Im-C<sub>18</sub>) for the preconcentration of trace heavy metals from aqueous samples as a prior step to their determination by inductively coupled plasma mass spectrometry (ICPMS). The material was characterized by Fourier-transform Infrared Spectroscopy (FTIR), Scanning Electron Microscopy (SEM), Thermogravimetric Analysis (TGA), Energy-Dispersive X-ray Spectroscopy (EDS), and Brunauer–Emmett–Teller (BET) analysis. A mini-column packed with SiO<sub>2</sub>-(CH<sub>2</sub>)<sub>3</sub>-Im-C<sub>18</sub> sorbent was used for the extraction of the metal ions complexed with 1-(2-pyridylazo)-2-naphthol (PAN) from the water sample. The effects of pH, PAN concentration, length of the alkyl chain of the ionic liquid, eluent concentration, eluent volume, and breakthrough volume have been investigated. The SiO<sub>2</sub>-(CH<sub>2</sub>)<sub>3</sub>-Im-C<sub>18</sub> allows the isolation and preconcentration of the heavy metal ions with enrichment factors of 150, 60, 80, 80, and 150 for Cr<sup>3+</sup>, Ni<sup>2+</sup>, Cu<sup>2+</sup>, Cd<sup>2+</sup>, and Pb<sup>2+</sup>, respectively. The limits of detection (LODs) for Cr<sup>3+</sup>, Ni<sup>2+</sup>, Cu<sup>2+</sup>, Cd<sup>2+</sup>, and Pb<sup>2+</sup> were 0.724, 11.329, 4.571, 0.112, and 0.819 μg L<sup>-1</sup>, respectively with the relative standard deviation (RSD) in the range of 0.941–1.351%.

 Received 11th May 2022  
 Accepted 30th June 2022

DOI: 10.1039/d2ra02980d

[rsc.li/rsc-advances](https://rsc.li/rsc-advances)

## 1. Introduction

Heavy metals have been widely used in various industries, including batteries, catalysts, dyes, textiles, paints, and cosmetics.<sup>1–3</sup> Heavy metals are considered one of the most common and hazardous pollutants in water due to the continuous increase of industry and other human activities.<sup>4,5</sup> Hence, metal content at the trace level in the environment has to be strongly regulated and controlled.<sup>6</sup> Main sources significantly contribute to the heavy metal contamination in the environment, including fossil fuel combustion, industrial plants, fertilizer usage. Especially, wastewaters were released from industrial zones containing heavy metals brings about a threat not only to aquatic life but also to the whole food chain.<sup>7,8</sup> Thus, it is essential to monitor and assess heavy metals pollution in water.

The sample preparation, including separation and preconcentration of the analytes, is a significant priority to gain accurate results in the analysis of heavy metal ions in water samples.<sup>9</sup> Extraction methods, including liquid–liquid extraction (LLE) and later solid-phase extraction (SPE), have been applied as effective sample pretreatment techniques to analyze metal at trace levels.<sup>10,11</sup> However, there are many disadvantages associated with liquid–liquid extraction, for example, incomplete phase separations, disposal of large quantities of organic solvent and manual performance.<sup>12</sup> Solid-phase extraction (SPE) provides a practical, reliable, and facile method for the preconcentration of heavy metals due to its low cost, high throughput, less organic solvent consumption, and automation ability.<sup>13</sup> SPE can be applied for a broader range of practical design situations than LLE because of the wide variety of sorbent chemistries, fast and automatic procedures.<sup>14</sup> Novel materials with various surface chemistries have been prepared, including modified silica,<sup>15–17</sup> graphene oxide,<sup>6,18,19</sup> imprinted polymers,<sup>20,21</sup> magnetic nanoparticles,<sup>22</sup> carbon nanotubes,<sup>23–25</sup> polymer,<sup>26,27</sup> and metal–organic framework<sup>28–30</sup> which applied as effective sorbents for the extraction of heavy metals.

Ionic liquids (ILs) are low melting point salts (below 100 °C), which are achieved mainly by bulky asymmetric cations and weakly coordinating anions.<sup>31,32</sup> They have attracted much attention due to their unique physical and chemical properties, including non-flammability, excellent conductivity, low vapor

<sup>a</sup>Department of Organic Chemistry, Faculty of Chemistry, University of Science, Ho Chi Minh City, Vietnam. E-mail: [thphuong@hcmus.edu.vn](mailto:thphuong@hcmus.edu.vn)

<sup>b</sup>Vietnam National University, Ho Chi Minh City, Vietnam. E-mail: [namai@hcmus.edu.vn](mailto:namai@hcmus.edu.vn)

<sup>c</sup>Center for Innovative Materials and Architectures (INOMAR), Ho Chi Minh City, Vietnam

<sup>d</sup>Department of Analytical Chemistry, Faculty of Chemistry, University of Science, Ho Chi Minh City, Vietnam

† Electronic supplementary information (ESI) available. See <https://doi.org/10.1039/d2ra02980d>



pressures, thermal stability, and designable structure.<sup>31,33,34</sup> ILs have emerged as potential candidates for sample preparation in several analytical determinations.<sup>35</sup> In the last decade, ILs can be tailored from a wide range of cations (tetraalkylammonium, imidazolium, morpholinium, oxazolidium, pyrrolidinium, piperidinium, piperazinium, pyridinium, phosphonium, sulfonium) and anions (chloride, bromide, hydrogensulfate, tosylate, hexafluorophosphate, and tetrafluoroborate) and thereby leading to the name of “designer solvents”. ILs are efficient sorbents for sample preparation because they can be designed to accomplish specific analytes.<sup>36</sup>

Silica porous materials have been used as supports in the preparation of sorbents due to their large specific surface areas and the ease of surface modification. Recently, IL-immobilized silica gels have been successfully used as efficient adsorbents in the SPE technique.<sup>31,37,38</sup> These sorbents can utilize as sorbents for sample preparation with a wide range of mechanisms of sorption, such as anion exchange, hydrogen bonding, and hydrophobic interactions.<sup>33</sup> Interestingly, these sorbents have been shown to be efficient sorbents for the separation of heavy metal ions.<sup>39,40</sup> Shemirani reported the use of [BMIM][PF<sub>6</sub>] (1-butyl-3-methylimidazolium hexafluorophosphate) immobilized onto silica gel as the sorbent for solid-phase extraction of Mn<sup>2+</sup>, Ni<sup>2+</sup>, Cd<sup>2+</sup>, Co<sup>2+</sup>, and Pb<sup>2+</sup> ions from tobacco and water samples before FAAS analysis. The IL-immobilized silica gel avoided the disadvantages of liquid-liquid extraction using ILs as extractants, such as slow mass transfer, excess amount of ILs, and leaching loss of ILs to the aqueous phase.<sup>41</sup> Thiol- and amino-functionalized ionic liquids were also shown great potential and high selectivity for the SPE of heavy metal ions without the use of complexing reagents.<sup>39,42–44</sup>

In the presented work, a new type of sorbent composed of silica gel and C18-alkylimidazolium ionic liquid immobilized silica (SiO<sub>2</sub>-(CH<sub>2</sub>)<sub>3</sub>-Im-C<sub>18</sub>) was firstly utilized for the simultaneous preconcentration of heavy metal cations in water samples. A novel C18-alkylimidazolium ionic liquid was prepared from imidazole as a starting material and immobilized onto silica with full characterizations. The material was developed for the preconcentration of Cr<sup>3+</sup>, Ni<sup>2+</sup>, Cu<sup>2+</sup>, Cd<sup>2+</sup>, and Pb<sup>2+</sup> ions in water samples and determination using inductively coupled plasma mass spectrometry (ICP-MS). In this procedure, the metal ions were first complexed with 1-(2-pyridylazo)-2-naphthol (PAN) in the water; the complexed metals were absorbed on the sorbent *via* electrostatic interaction. The present method, which was proved to be rapid, efficient, and convenient in sample preparation, could be potentially applied to separate and enrich trace amounts of Cr<sup>3+</sup>, Ni<sup>2+</sup>, Cu<sup>2+</sup>, Cd<sup>2+</sup>, and Pb<sup>2+</sup> ions from water samples.

## 2. Experimental section

### 2.1. Chemical and instrumentation

Silica gel 230–400 mesh (37–63 μm) was purchased from Himedia (India). Imidazole (≥99%), 1-bromooctane (≥97%), 1-bromooctadecane (≥97%), 1-methylimidazole (≥99%), (3-chloropropyl)triethoxysilane (≥95%), sodium hydroxide (>85%), sodium chloride (≥99%), polyethylene glycol *tert*-

octylphenyl ether (Triton X-100) were purchased from Sigma-Aldrich.

Stock standard solutions (1000 mg L<sup>-1</sup> in HNO<sub>3</sub> 0.5 mol L<sup>-1</sup>) of Pb<sup>2+</sup>, Cd<sup>2+</sup>, Cu<sup>2+</sup>, Ni<sup>2+</sup>, Cr<sup>3+</sup> with were obtained from Merck. Working standard solutions were prepared by proper dilutions of stock standard solutions. 1-(2-Pyridylazo)-2-naphthol (PAN), sulfuric acid (≥97.5%), hydrochloric acid (37% in H<sub>2</sub>O), nitric acid (70% in H<sub>2</sub>O), ethanol (anhydrous, ≥ 99%), acetonitrile (anhydrous, ≥ 99.8%), toluene (anhydrous, ≥ 99%), methanol (anhydrous, ≥ 99%) were obtained from Merck. Deionized water was prepared by a Milli-Q system.

The reactions in this experiment were conducted on an IKA C-MAG HS7 magnetic stirrer. FT-IR spectra were recorded on a Bruker E400 spectrometer using potassium bromide pellets. Adjustment of pH was performed with Mettler-Toledo pH InLab®Expert Pro-ISM electrode. TGA was measured on a TA Q500 thermal analysis system with a temperature ramp of 5 °C min<sup>-1</sup> under airflow. The morphology of materials was observed on XZS – 107T digital microscope coupling with NHV – CAM using eScope software and Hitachi S-4800 scanning electron microscope (SEM). The N<sub>2</sub> isotherm measurements were carried out at 77 K on Quantachrome NOVA 3200e system. Energy-dispersive X-ray spectroscopy (EDX) analysis was recorded using an EMAX energy EX-400 EDX device to determine the element contents of sorbents. The concentrations of heavy metal ions were determined by inductively coupled plasma mass spectrometry (Agilent ICP-MS 7700x instrument).

### 2.2. Synthetic procedure of ionic liquid-grafted silica gel SiO<sub>2</sub>-(CH<sub>2</sub>)<sub>3</sub>-Im-C<sub>18</sub>

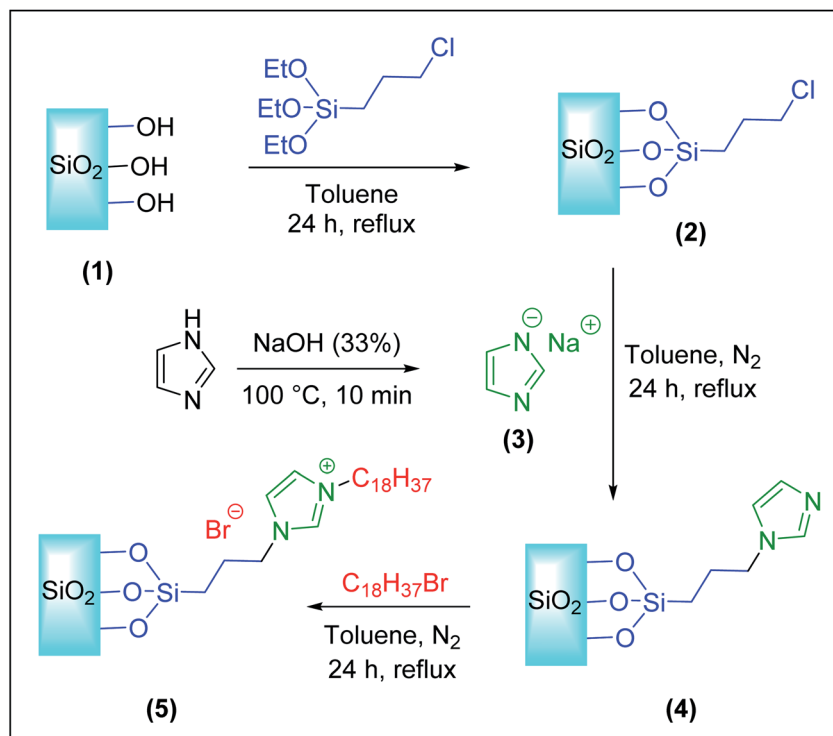
The silica-supported ionic liquids SiO<sub>2</sub>-(CH<sub>2</sub>)<sub>3</sub>-Im-C<sub>18</sub> was synthesized *via* a four-step procedure presented in Scheme 1 as follows:

**2.2.1. Activation silica gel (1).** Silica gel was activated to enhance the content of silanol groups on the silica surface. The mixture of silica gel (5.5 g) and nitric acid (5.5 g) (1 : 1, w/w) was refluxed at 80 °C for 4 h to activate the silica gel surface and eliminate metal oxide. After washing with distilled water, the activated silica gel was recovered by filtration and washed with distilled water until reached pH 7.0 and dried at 120 °C for 24 h.

**2.2.2. Synthesis of SiO<sub>2</sub>-(CH<sub>2</sub>)<sub>3</sub>-Cl (2).** The second step was the preparation of 3-chloropropyl silica (2). The mixture of (3-chloropropyl)triethoxysilane (42.5 mmol, 10.2 g) and activated silica gel (10.0 g) in toluene (10 mL) was dispersed for 15 min under ultrasonic irradiation and then heated to reflux for 24 h. After the completion of the reaction, 3-chloropropyl silica was recovered by filtration, washed with acetone (5 × 20 mL), and centrifuged at 1000 rpm for 10 min. The resulting material was dried under vacuum at 80 °C for 3 h to provide the desired 3-chloropropyl silica (2).

**2.2.3. Synthesis of sodium imidazolide (3).** Sodium imidazolide (3) was prepared by the deprotonation of imidazole according to the following procedure. Imidazole (10 mmol, 0.68 g) was added to sodium hydroxide 33% (10 mmol, 0.4 g). The mixture was stirred to afford a homogeneous solution and then



Scheme 1 Synthetic procedure of  $\text{SiO}_2-(\text{CH}_2)_3\text{-Im-C}_{18}$ .

heated for 15 min at 100 °C. The solution was cooled and evaporated to dryness, and the remaining solid was dried at 75 °C for 1 h to give the sodium salt as a crystalline powder.

**2.2.4. Synthesis of  $\text{SiO}_2-(\text{CH}_2)_3\text{-Im}$  (4).** The vital step in this procedure is the nucleophilic addition of the 3-chloropropyl silica (2) with sodium imidazolate (3) to produce 3-(1-imidazole)propyl silica (4). 3-Chloropropyl silica (5.0 g) and sodium imidazolate (10 mmol, 0.9 g) were added to a 100 mL round-bottomed flask with 30 mL anhydrous toluene. The mixture was refluxed for 24 h in an oil bath under an inert atmosphere. After completion, the obtained solid was filtrated and washed several times with ethanol ( $5 \times 20$  mL). The purified product was dried under a vacuum for the next step.

**2.2.5. Synthesis of  $\text{SiO}_2-(\text{CH}_2)_3\text{-Im-C}_{18}$  (5).**  $\text{SiO}_2-(\text{CH}_2)_3\text{-Im}$  (4) (3.1 g) was added to 100 ml of a toluene solution containing 10 mmol of 1-bromooctadecane and stirred vigorously for 15 min. The reaction mixture was heated at 120 °C for 24 h. Upon completion, the resulting product was collected from the solution mixture by filtration and rinsed several times with ethanol and water. The purified product was dried under reduced pressure at 100 °C for 12 h to afford silica-supported ionic liquids ( $\text{SiO}_2-(\text{CH}_2)_3\text{-Im-C}_{18}$ ).

### 2.3. Preparation of column

0.2 g of the silica-supported ionic liquid material ( $\text{SiO}_2-(\text{CH}_2)_3\text{-Im-C}_{18}$ ) was added to empty cartridges (6.0 cm length, 0.9 cm internal diameter). Frit was plugged at the ends of cartridges to keep the sorbent inside the tube (please see Fig. S1 in ESI†). Before its application, the SPE column was cleaned and

conditioned by passing with 1 mol  $\text{L}^{-1}$   $\text{HNO}_3$  in methanol solution (10 mL) followed by deionized water (10 mL).

### 2.4. General procedure for solid-phase extraction

From 1000 mg  $\text{L}^{-1}$  stock solutions of 5 metal ions ( $\text{Pb}^{2+}$ ,  $\text{Cd}^{2+}$ ,  $\text{Cu}^{2+}$ ,  $\text{Ni}^{2+}$ ,  $\text{Cr}^{3+}$ ), the working standard mixture containing 50  $\mu\text{g L}^{-1}$  each was freshly prepared by successive dilutions. The  $\text{SiO}_2-(\text{CH}_2)_3\text{-Im-C}_{18}$  cartridge was first cleaned, preconditioned with 10 mL of  $\text{HNO}_3$  in methanol (1 M) and 10 mL of deionized water. Standard solution (50 mL) containing metal ions (50  $\mu\text{g L}^{-1}$ ) and PAN was adjusted to pH 8.5 using buffer solution and loaded on the conditioned column at a flow rate of 0.8 mL  $\text{min}^{-1}$ . Subsequently, the metal complexes were eluted from the column using 1 mL  $\text{HNO}_3$  in ethanol (1 M), filtered through a syringe filter 0.45  $\mu\text{m}$ , and determined by ICP-MS. A blank solution was also subjected to the same procedure without adding any standard solutions and used as a control.

## 3. Results and discussion

### 3.1. Characterization of silica-supported ionic liquids $\text{SiO}_2-(\text{CH}_2)_3\text{-Im-C}_{18}$

The ionic liquid immobilized onto silica was synthesized according to the detailed procedure as described in the experimental section (Scheme 1). The structural and morphological properties of the product were confirmed by FTIR, TGA, SEM, EDX, and BET. The chemical immobilization of ILs onto silica was formed through Si-O-Si bridges. The FT-IR spectrum of compound (2) had been described by Adam and coworkers.<sup>45</sup>



The absorption peaks of the silica shell in the sorbent around  $1054\text{ cm}^{-1}$  and  $797\text{ cm}^{-1}$  were attributed to the antisymmetric and symmetric signals of Si–O–Si bond. Moreover, the band at  $1631\text{ cm}^{-1}$  was also attributed to the Si–OH group. Besides, the alkyl group was also confirmed by absorption peak of the C–H bond at  $2923\text{ cm}^{-1}$  (Fig. 1b) and the weak peak in the region of  $800\text{--}630\text{ cm}^{-1}$  could be assigned to C–Cl stretching.<sup>45</sup> The synthesis of compound (4) through the alkylation of compound (2) with sodium imidazolid (3) was carried out by a similar procedure reported by Amarasekara *et al.*<sup>46</sup> and Kotadia *et al.*<sup>47</sup> The peak at  $1667\text{ cm}^{-1}$  and  $3016\text{ cm}^{-1}$  was observed, which was caused by vibration of the imidazole ring (Fig. 1c).<sup>46,47</sup> Based on the result of Fig. 1d, it could be seen that two sharp peaks of at  $2917\text{--}2849\text{ cm}^{-1}$  and one peak at  $1465\text{ cm}^{-1}$  were observed, corresponding to the C–H stretch of the added hydrocarbon chain. Similar signals of FTIR spectrum of C18-alkyl chain grafted onto multiwalled carbon nanotubes was reported by Li and Greenberg.<sup>48</sup> The above data indicated that the long-chain C18-alkyl imidazolium ionic liquid was successfully immobilized on activated silica gel.

The stability and the mass of ionic liquid coating on the surface of the active silica gel were determined by the thermal gravimetric analysis method (Fig. 2). The measurement was carried out in the  $25\text{--}800\text{ }^{\circ}\text{C}$  temperature range, with a heating rate of  $5\text{ }^{\circ}\text{C min}^{-1}$  under an air atmosphere.  $\text{SiO}_2\text{-(CH}_2\text{)}_3\text{-Im-C}_{18}$  showed a slight decrease in weight ( $\sim 7.5\%$ ) below  $100\text{ }^{\circ}\text{C}$ , attributed to the evaporation of the solvent and  $\text{H}_2\text{O}$  residues. The sharp decrease in weight ( $\sim 13\%$ ) from  $200$  to  $600\text{ }^{\circ}\text{C}$  was attributed to an organic compound corresponding to the ionic liquid. The data of TGA of  $\text{SiO}_2\text{-(CH}_2\text{)}_3\text{-Im-C}_{18}$  could be compared with the similar ionic liquid grafted onto silica reported by Amarasekara and Owereh.<sup>46</sup> The thermal gravimetric

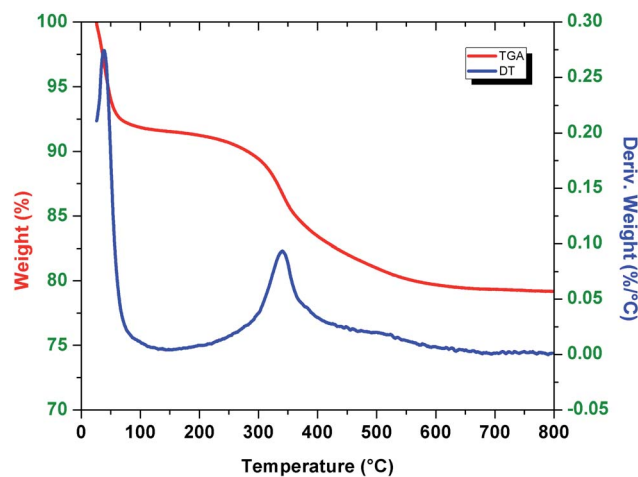


Fig. 2 Thermal gravimetric analysis diagram of  $\text{SiO}_2\text{-(CH}_2\text{)}_3\text{-Im-C}_{18}$ .

analysis indicated the successful synthesis of ionic liquid-grafted silica gel.

The elemental content of the ionic liquid-functionalized silica gel surface was evaluated by energy-dispersive X-ray spectroscopy (EDX). The EDX diagram confirmed the presence of carbon, nitrogen, oxygen, silicon, and bromine elements in the structure of this sorbent, indicating the successful coating of ionic liquids onto the silica gel surface (Fig. 3).

As depicted in Fig. 4, the morphology of the ionic liquid-immobilized silica gel was studied using SEM characterization. The as-prepared  $\text{SiO}_2\text{-(CH}_2\text{)}_3\text{-Im-C}_{18}$  had not a regular sphere morphology but a very sharp-cut and rough surface. The results suggested that the ionic liquid immobilized onto silica affected the morphology of the silica. The SEM image of  $\text{SiO}_2\text{-(CH}_2\text{)}_3\text{-Im-C}_{18}$  revealed that the material was obtained in

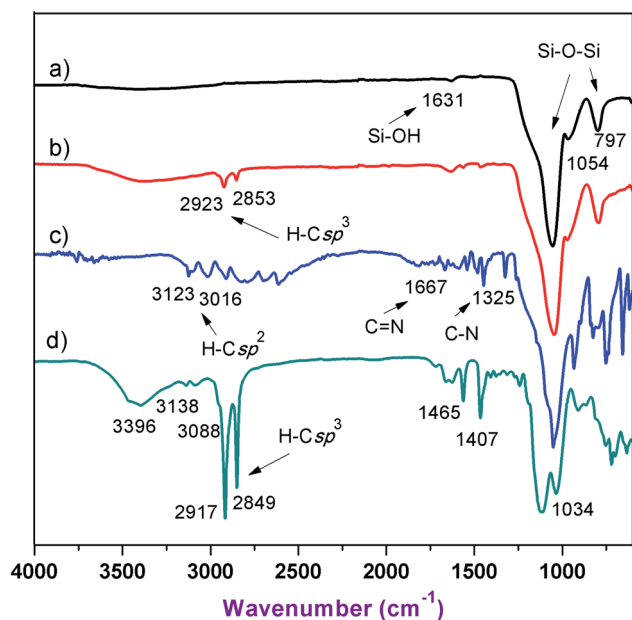


Fig. 1 FT-IR spectra of (a)  $\text{SiO}_2$  (1), (b)  $\text{SiO}_2\text{-(CH}_2\text{)}_3\text{-Cl}$  (2), (c)  $\text{SiO}_2\text{-(CH}_2\text{)}_3\text{-Im}$  (4), (d)  $\text{SiO}_2\text{-(CH}_2\text{)}_3\text{-Im-C}_{18}$  (5).

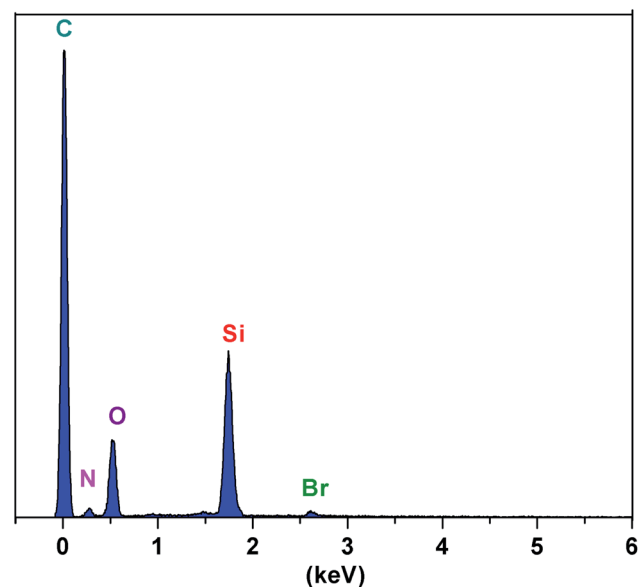


Fig. 3 Energy-dispersive X-ray spectroscopy of  $\text{SiO}_2\text{-(CH}_2\text{)}_3\text{-Im-C}_{18}$ .



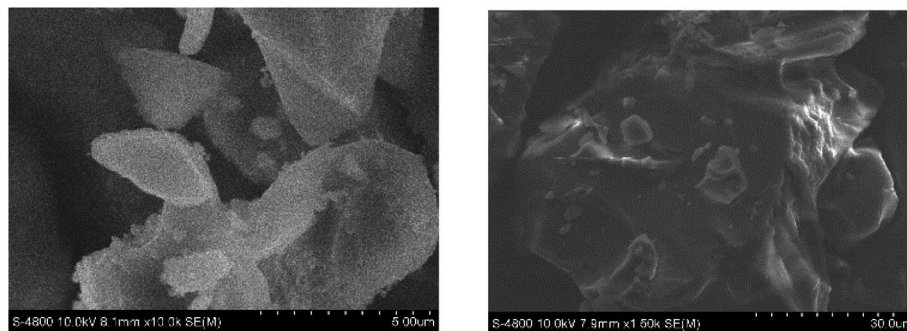


Fig. 4 SEM image of  $\text{SiO}_2-(\text{CH}_2)_3\text{-Im-C}_{18}$ .

micrometer-sized particles and indicated further evidence for the successful preparation of  $\text{SiO}_2-(\text{CH}_2)_3\text{-Im-C}_{18}$ .

Based on the  $\text{N}_2$  sorption isotherm at 77 K, the BET-specific surface area of  $\text{SiO}_2-(\text{CH}_2)_3\text{-Im-C}_{18}$  sorbent was  $330 \text{ m}^2 \text{ g}^{-1}$  with average half pore width of  $18 \text{ \AA}$ . As seen in Fig. 5, the immobilization of ionic liquid on silica decreased the surface area of the original silica gel ( $450 \text{ m}^2 \text{ g}^{-1}$ ). Moreover, the half pore width and pore volume of silica-supported ionic liquids were lower than bare silica gel (Table 1). The results suggested that the ionic liquid immobilized onto silica gel was successfully prepared.

### 3.2. Optimization of analytical conditions

**3.2.1. Effect of sample pH on sorption efficiency.** The sorbent did not retain the pure metal ions, so the popular reagent PAN was chosen to complex with metal ions.<sup>49–53</sup> The pH of sample solutions, which has a significant impact on the stability of the metal-PAN complexes, is one of the essential factors for efficient retention of the metal ions on the sorbent. To find the optimal pH for simultaneous extraction of the metal ions from aqueous samples, pH was varied in the range of 4.5–9.5 using buffers prepared from borax and sodium hydroxide or

Table 1 Surface area, half pore width and pore volume comparison of silica-supported ionic liquids and bare silica gel

Material	Specific surface area ( $\text{m}^2 \text{ g}^{-1}$ )	Half pore width ( $\text{\AA}$ )	Pore volume ( $\text{cm}^3 \text{ g}^{-1}$ )
Silica gel	450	26	0.750
$\text{SiO}_2-(\text{CH}_2)_3\text{-Im-C}_{18}$	330	18	0.469

hydrochloric acid ( $0.1 \text{ mol L}^{-1}$ ). The sorption percentage of metal ions was calculated based on the difference between the concentration of metal ions in the initial solution and the solution out flowing from the SPE column (Fig. 6). It was evident that the sorption of all metal ions on the  $\text{SiO}_2-(\text{CH}_2)_3\text{-Im-C}_{18}$  increased with the rising of pH and reached the maximum at pH 8.5. The low efficiency of the sorption was observed at  $\text{pH} < 7.5$  due to the unstable metal-PAN complex. All subsequent work was, therefore, carried out at the optimum pH of 8.5.

**3.2.2. Effect of PAN concentration.** PAN, an orange-colored dye, acts as a tridentate ligand and can form stable chelate complexes between metal ions with its oxygen atom and azo

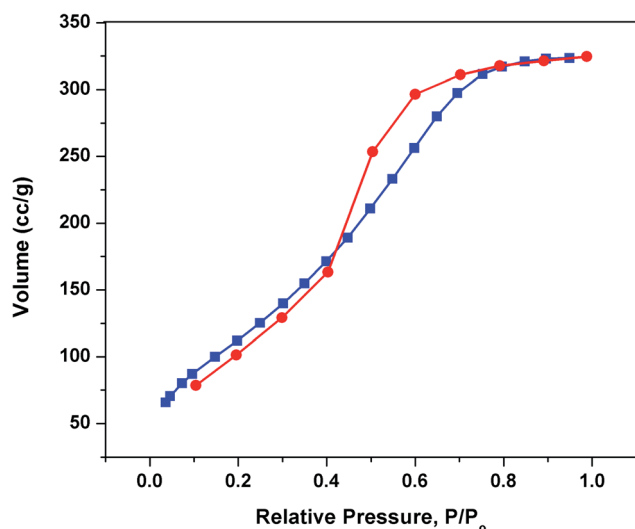


Fig. 5 BET of  $\text{SiO}_2-(\text{CH}_2)_3\text{-Im-C}_{18}$ .

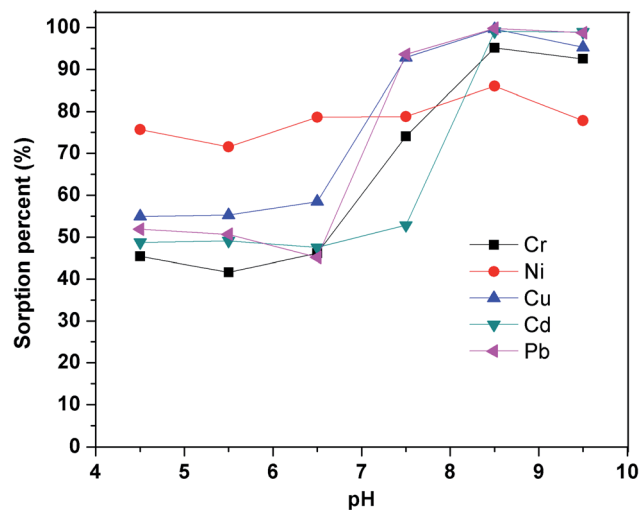


Fig. 6 Effect of pH on the sorption percentage. Utilized conditions:  $\text{Cr}^{3+}$ ,  $\text{Ni}^{2+}$ ,  $\text{Cu}^{2+}$ ,  $\text{Cd}^{2+}$ , and  $\text{Pb}^{2+}$   $50 \mu\text{g L}^{-1}$ ; volume:  $50 \text{ mL}$ ; PAN:  $2 \times 10^{-5} \text{ mol L}^{-1}$ ; flow rate:  $0.8 \text{ mL min}^{-1}$ .



group. The effect of PAN concentration on the sorption percent of metal ions from the aqueous solution was studied from  $1 \times 10^{-5}$  to  $8 \times 10^{-5}$  mol L<sup>-1</sup>. As seen in Fig. 7, maximum sorption was obtained at a PAN concentration of  $2 \times 10^{-5}$  mol L<sup>-1</sup> with the metal ions. The decreased sorption efficiency at higher PAN concentrations could be explained due to the competition for adsorbing sites by the excess ligand with the sorbent. Thus, a concentration of  $2 \times 10^{-5}$  mol L<sup>-1</sup> of PAN was chosen for the following experiments.

**3.2.3. Effect of length of alkyl chain.** Two other silica-supported ionic liquids with very short (C1) and medium (C8) alkyl chains were prepared by the same procedure as for SiO<sub>2</sub>-(CH<sub>2</sub>)<sub>3</sub>-Im-C<sub>18</sub> (please see Sections S2 and S3 in the ESI†). Among these, the SiO<sub>2</sub>-(CH<sub>2</sub>)<sub>3</sub>-Im-C<sub>18</sub> provided the best sorption under optimized conditions (Fig. 8). The silica gel without ionic liquid showed very low sorption of heavy metal ions. The low efficiency of bare silica and the two sorbents with short alkyl chains (C-1 and C-8) was obtained presumably due to the weaker hydrophobic interactions between the sorbents and aromatic moieties of PAN complexes.

**3.2.4. Effect of concentration of eluent.** Various eluents, including methanol, HCl in ethanol, HNO<sub>3</sub> in ethanol, and H<sub>2</sub>SO<sub>4</sub> in methanol, were investigated. Among these, HNO<sub>3</sub> in ethanol showed the best eluent. Thus, the concentration of nitric acid in ethanol was investigated in the range from 0.5 mol L<sup>-1</sup> to 2.0 mol L<sup>-1</sup> at a flow rate of 0.8 mL min<sup>-1</sup>. The eluent volume should be taken with the smallest volume for gaining a high preconcentration factor. As shown in Fig. 9, low recoveries of Cr<sup>3+</sup> and Pb<sup>2+</sup> were observed when 1 mL HNO<sub>3</sub> (0.5 mol L<sup>-1</sup>) was used as eluent. 1 mL HNO<sub>3</sub> (2 mol L<sup>-1</sup>) provided a quantitative recovery of metal ions (from 75 to 100%). The increase of eluent volume to 2 mL or 5 mL did not improve the recovery of metal ions. Therefore, 1.0 mL HNO<sub>3</sub> eluent 2 mol L<sup>-1</sup> was used in the following experiments.

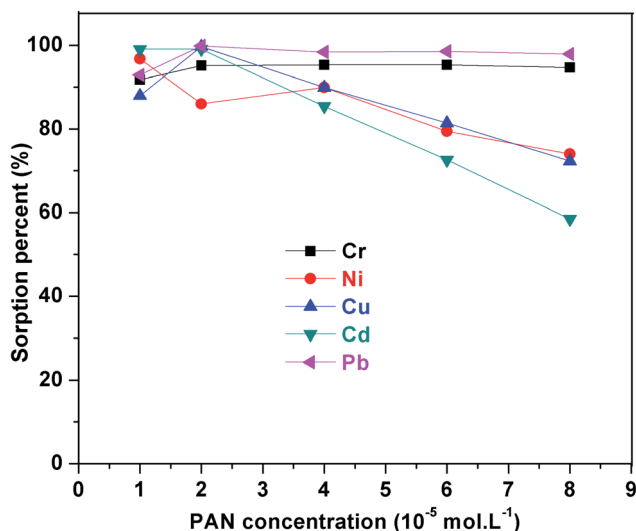


Fig. 7 Effect of PAN concentration on SiO<sub>2</sub>-(CH<sub>2</sub>)<sub>3</sub>-Im-C<sub>18</sub>. Utilized conditions: Cr<sup>3+</sup>, Ni<sup>2+</sup>, Cu<sup>2+</sup>, Cd<sup>2+</sup>, and Pb<sup>2+</sup> 50 µg L; volume: 50 mL; flow rate: 0.8 mL.min<sup>-1</sup>.

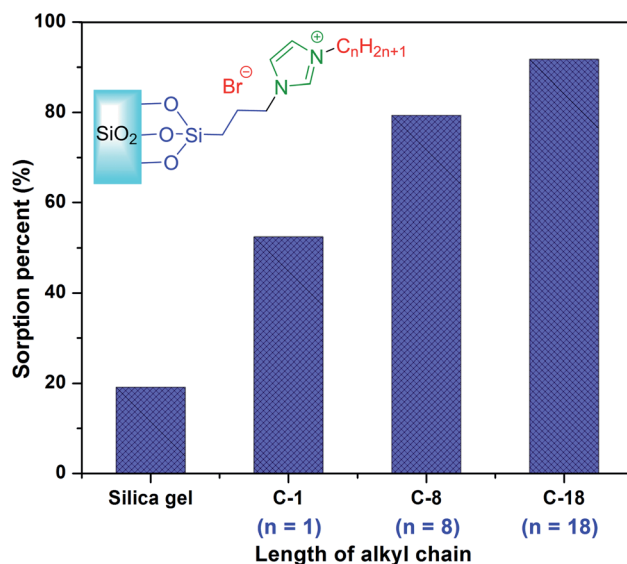


Fig. 8 Effect of the length of alkyl chain.

**3.2.5. Breakthrough volume.** Breakthrough volume, the maximum volume of sample, which can be optimized into a sorbent without significant leak of analytes, is usually one of the important parameters in SPE. Together with the required eluent volume to quantitatively elute analytes, breakthrough volume determines the enrichment factor of the material. It is especially of great concern when dealing with trace levels. The breakthrough volume of aqueous samples containing Cr<sup>3+</sup>, Ni<sup>2+</sup>, Cu<sup>2+</sup>, Cd<sup>2+</sup>, and Pb<sup>2+</sup> (50 µg L<sup>-1</sup> each) was evaluated by monitoring the sorption percent while increasing sample volumes over the range of 10–150 mL at the optimal conditions. The maximum loading volume was found to be 60 mL without significant leaching of five ions. As seen in Fig. 10, the sorption was found to be stable until 150 mL with Cr<sup>3+</sup> and Pb<sup>2+</sup>. Thus, with the optimized 1.0 mL HNO<sub>3</sub> elution, the preconcentration factor was found as 150 for Cr<sup>3+</sup> and Pb<sup>2+</sup> ion. The sorption of Ni<sup>2+</sup>, Cu<sup>2+</sup>, Cd<sup>2+</sup> was found to be stable with 60 mL, 80 mL, 80 mL, respectively. Hence, the preconcentration factors were found as 60, 80, 80 for Ni<sup>2+</sup>, Cu<sup>2+</sup>, Cd<sup>2+</sup> ions.

**3.2.6. Detection limits and precision.** Under the optimized experimental conditions, the calibration curves for Cr<sup>3+</sup>, Ni<sup>2+</sup>, Cu<sup>2+</sup>, Cd<sup>2+</sup>, and Pb<sup>2+</sup> were linear in the concentration range from 0.1 µg L<sup>-1</sup> to 50 µg L<sup>-1</sup> with high correlation coefficients from 0.9998 to 1. The quantitative characteristics of the present method, including LOD, LOQ, and RSD, were studied and the results were summarized in Table 2. To evaluate the precision of the method, eleven replicates were carried out, and the RSDs were calculated. As seen in Table 2, the RSD values of the method are about 0.9–1.3%, indicating that the proposed process is repeatable. The low LOD and LOQ could be achieved with the exception of Ni<sup>2+</sup> ion. This material was not favorable for the extraction of Ni<sup>2+</sup> ion, presumably due to the low interaction of Ni<sup>2+</sup> ion with PAN.

**3.2.7. Matrix effect.** The interference could affect the preconcentration step. The cations could react with ligand and



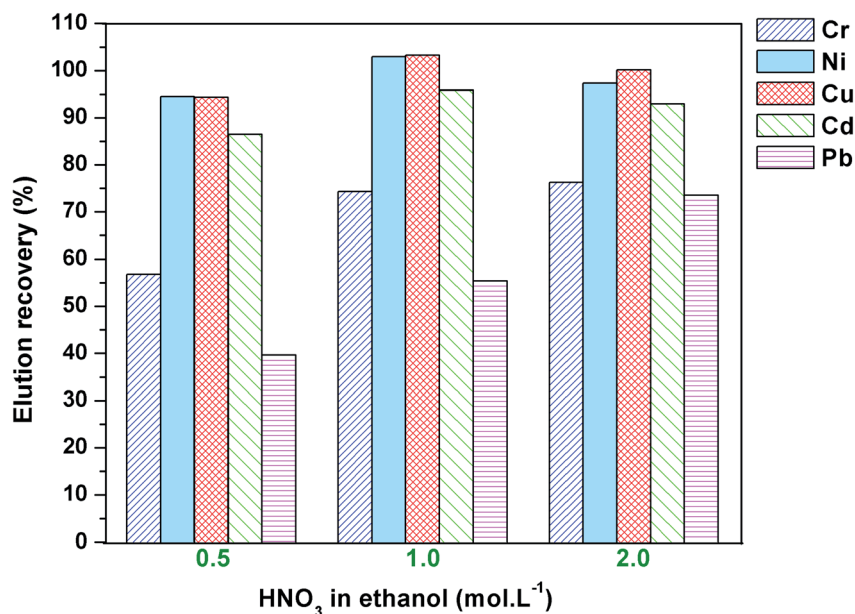


Fig. 9 Effect of nitric acid concentration on the elution recovery.

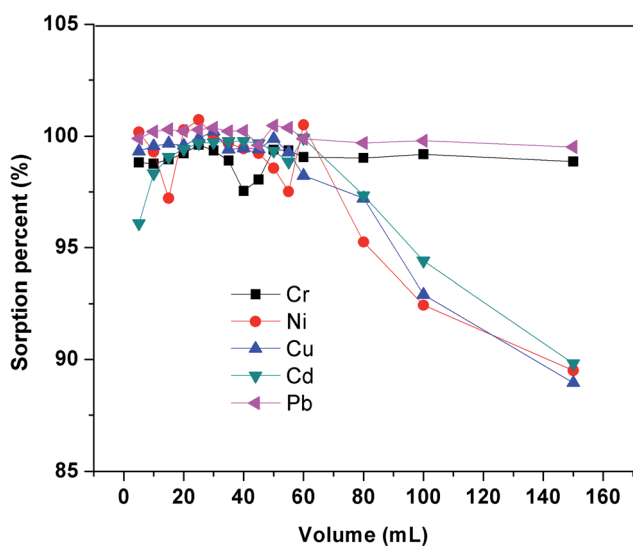


Fig. 10 Effect of sample volume on sorption percent.

Table 2 Quantitative characteristics of the present method

Analyte	LOD ( $\mu\text{g L}^{-1}$ )	LOQ ( $\mu\text{g L}^{-1}$ )	RSD (%)
Cr	0.724	2.173	1.133
Ni	11.329	33.988	1.142
Cu	4.571	13.711	1.351
Cd	0.112	0.335	0.941
Pb	0.819	2.459	1.195

anions also formed the stable complex with metal ions, leading to decrease metal ion recoveries. Table 3 showed minimal change in recoveries of analytes with a high concentration of

Table 3 Effects of the interfering ions on the recoveries of the metal ions

Ion	Added salt	Ratio [coexisting ion]/[metal ion]	Recovery (%)				
			Cr	Ni	Cu	Cd	Pb
Na <sup>+</sup>	Na <sub>2</sub> CO <sub>3</sub>	500	67.7	97.0	103.3	98.8	65.0
K <sup>+</sup>	KCl	500	54.7	75.8	78.0	73.3	58.5
Ca <sup>2+</sup>	CaCl <sub>2</sub>	500	58.1	71.5	73.4	100.2	65.5
Mg <sup>2+</sup>	MgSO <sub>4</sub>	500	81.5	96.6	99.6	93.6	68.9
Cl <sup>-</sup>	KCl	450	54.7	75.8	78.0	73.3	58.5
SO <sub>4</sub> <sup>2-</sup>	MgSO <sub>4</sub>	2000	81.5	96.6	99.6	93.6	68.9
CO <sub>3</sub> <sup>2-</sup>	Na <sub>2</sub> CO <sub>3</sub>	650	67.7	97.0	103.3	98.8	65.0

matrices salts. Cations (Na<sup>+</sup>, K<sup>+</sup>, Ca<sup>2+</sup>, Mg<sup>2+</sup>) and anion (Cl<sup>-</sup>, SO<sub>4</sub><sup>2-</sup>, CO<sub>3</sub><sup>2-</sup>) are present in natural waters and affect the sorption and extraction. Thus, the effect of various salts, including Na<sub>2</sub>CO<sub>3</sub>, KCl, CaCl<sub>2</sub>, and MgSO<sub>4</sub> on the Cr<sup>3+</sup>, Ni<sup>2+</sup>, Cu<sup>2+</sup>, Cd<sup>2+</sup>, Pb<sup>2+</sup> recovery was studied. As shown in Table 3, the recovery of metal ions did not decrease significantly in the presence of 500-fold excess of Na<sup>+</sup>, Mg<sup>2+</sup> or 650-fold excess of CO<sub>3</sub><sup>2-</sup>, 2000-fold excess SO<sub>4</sub><sup>2-</sup>, whereas a slight reduction in the recoveries (10–15%) was observed in the presence of 500-fold excess K<sup>+</sup> or 450-fold excess Cl<sup>-</sup>.

**3.2.8. Application to real water samples.** In order to demonstrate the validity of the C18-alkylimidazolium ionic liquid immobilized silica sorbent (SiO<sub>2</sub>-(CH<sub>2</sub>)<sub>3</sub>-Im-C<sub>18</sub>) under the optimum experimental conditions, river water and tap water samples were used for preconcentration and determination of Cr<sup>3+</sup>, Ni<sup>2+</sup>, Cu<sup>2+</sup>, Cd<sup>2+</sup>, and Pb<sup>2+</sup> by ICPMS. The method precision was evaluated using spiked water samples, and the recovery experiments of different amounts of heavy metal ions were employed. Based on Fig. 11, these results indicated that



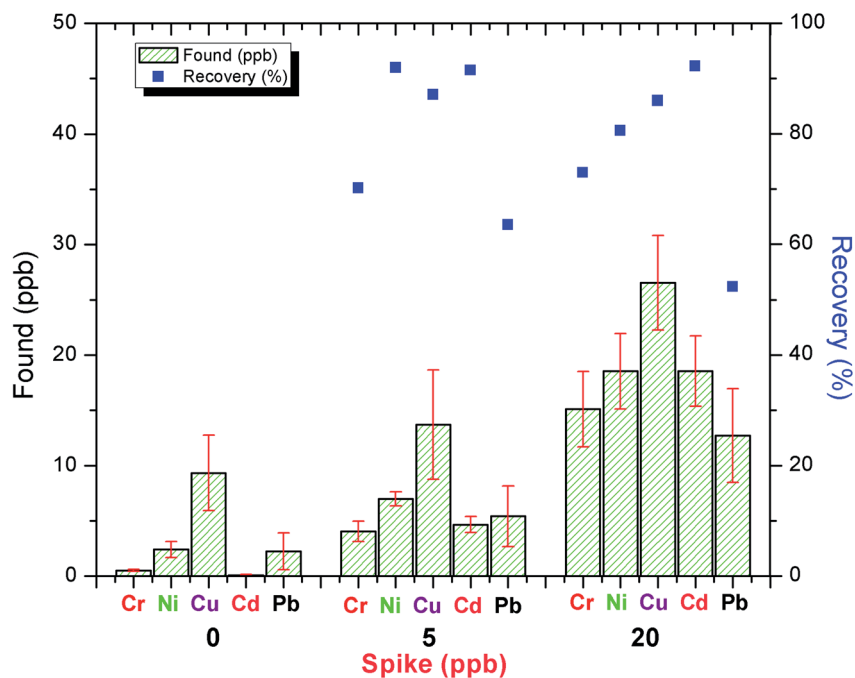


Fig. 11 Determination of  $\text{Cr}^{3+}$ ,  $\text{Ni}^{2+}$ ,  $\text{Cu}^{2+}$ ,  $\text{Cd}^{2+}$ , and  $\text{Pb}^{2+}$  in water samples. Average of three determinations  $\pm$  standard deviation (SD),  $n = 3$ .

Table 4 Comparison of sorption performances of the present study and other reported literature

Sorbent	Element	Enrichment factor	LOD ( $\mu\text{g L}^{-1}$ )	RSD (%)
Polyethylene glycol loaded on silica gel ( $\text{SiO}_2@\text{PEG}$ ) <sup>54</sup>	Cu(II), Cd(II), Mn(II)	66.6	0.33–1.20	3.42–4.91
Dithioamide onto activated carbon ( $\text{AC}@\text{DTO}$ ) <sup>55</sup>	Ni(II), Co(II), Cu(II)	330	0.5–0.8	<2
1-(2-Pyridylazo)-2-naphthol loaded on silica gel ( $\text{SiO}_2@\text{PAN}$ ) <sup>56</sup>	Cr(III), Mn(II), Fe(III), Ni(II), Cu(II), Cd(II), Pb(II)	80–150	0.13–4.1	5–26
Thiosalicylic acid loaded on silica gel <sup>57</sup>	Pb(II)	150	3.7	<1.5
Dihydroxybenzene loaded on silica gel <sup>58</sup>	Cu(II), Pb(II), Fe(III), Zn(II), Co(II), Ni(II), Cd(II)	250	4	1.4–7.0
Amberlite XAD-2010 resin <sup>59</sup>	Mn(II), Co(II), Ni(II), Cu(II), Cd(II), Pb(II)	100	0.08–0.26	1.9–5.1
This work: ( $\text{SiO}_2-(\text{CH}_2)_3\text{-Im-C}_{18}$ )	Cr(III), Ni(II), Cu(II), Cd(II), Pb(II)	60–150	0.724–11.329	0.941–1.351

the recoveries were reasonable for trace analysis in the real water sample.

**3.2.9. Comparison with the previous literature.** The analysis performance of the current method was compared with previous sorbents reported earlier in the literature. Table 4 showed the comparison data of the current method with previous literature. The enrichment factor values were reported in the previous literature range from 66 to 330 depending on the sorbents, and our material also reaches from 60 to 150. Our method can be attributed to the new *N*-octyldecylimidazolium ionic liquid-immobilized silica sorbent, which exhibits a high extraction of  $\text{Cr}^{3+}$ ,  $\text{Cu}^{2+}$ ,  $\text{Cd}^{2+}$ , and  $\text{Pb}^{2+}$ . Some parameters

obtained by our work are comparable to those presented by other methods described in the previous literature.

## 4. Conclusions

An efficient procedure for the synthesis of a new *N*-octyldecylimidazolium ionic liquid-immobilized silica sorbent was developed. The characterization of ionic liquid-immobilized silica sorbent was carried out by FTIR, SEM, TGA, BET, and EDX. The as-synthesized ionic liquid-immobilized silica sorbent exhibits effective extraction with good enrichment factor for the  $\text{Cr}^{3+}$ ,  $\text{Ni}^{2+}$ ,  $\text{Cu}^{2+}$ ,  $\text{Cd}^{2+}$ , and  $\text{Pb}^{2+}$ , making the sorbent very suitable for



SPE of trace heavy metals in the water sample. This research proved that the porous silica material has been used as support in the preparation of sorbents due to their large specific surface areas and the ease of surface modification. The IL-grafted silica has showed the efficient sorbent towards metal-PAN complexes in the SPE technique. The results demonstrated that the method could be effectively used as an alternative method for the simultaneous determination of heavy metal ions in water samples.

## Author contributions

The Thai Nguyen, Tu-Hoai Duy Nguyen, Tam Thanh Thi Huynh: conceptualization, methodology, data curation, formal analysis, validation. Minh-Huy Dinh Dang, Thuy-Linh Ho Nguyen, Tan Hoang Le Doan: material analysis, data curation, review editing. Thinh Phuc Nguyen, Mai Anh Nguyen: supervision, review, and editing. Phuong Hoang Tran: conceptualization, supervision, writing, review, and editing.

## Conflicts of interest

The authors have no conflicts to declare.

## Acknowledgements

We are grateful to the Ho Chi Minh Department of Science and Technology (grant no. 102/2020/HĐ-QPTKHCN) for financial support.

## References

- 1 Y.-K. Li, T. Yang, M.-L. Chen and J.-H. Wang, *Crit. Rev. Anal. Chem.*, 2021, **51**, 353–372.
- 2 S. Bolisetty, M. Peydayesh and R. Mezzenga, *Chem. Soc. Rev.*, 2019, **48**, 463–487.
- 3 F. Lu and D. Astruc, *Coord. Chem. Rev.*, 2018, **356**, 147–164.
- 4 C. Mohod and J. Dhote, *Int. J. Innov. Res. Sci. Eng.*, 2013, **2**, 2992–2996.
- 5 M. L. Sall, A. K. D. Diaw, D. Gningue-Sall, S. Efremova Aaron and J.-J. Aaron, *Environ. Sci. Pollut. Res.*, 2020, **27**, 29927–29942.
- 6 X. Dong, X. Gao, J. Song and L. Zhao, *Food Chem.*, 2021, **360**, 130023.
- 7 L. N. Sibal and M. P. B. Espino, *Int. J. Environ. Anal. Chem.*, 2018, **98**, 536–554.
- 8 C. Liu, Q. Wang, F. Jia and S. Song, *J. Mol. Liq.*, 2019, **292**, 111390.
- 9 T. Liu and J. Chen, *Sep. Purif. Technol.*, 2021, **276**, 119263.
- 10 Y. A. Zolotov, N. M. Kuz'min, O. M. Petrukhin and B. Y. Spivakov, *Anal. Chim. Acta*, 1986, **180**, 137–161.
- 11 B. Buszewski and M. Szultka, *Crit. Rev. Anal. Chem.*, 2012, **42**, 198–213.
- 12 S. Büyüktiryaki, R. Keçili and C. M. Hussain, *TrAC, Trends Anal. Chem.*, 2020, **127**, 115893.
- 13 B. Hashemi and S. Rezaia, *Microchim. Acta*, 2019, **186**, 578.
- 14 A. Andrade-Eiroa, M. Canle, V. Leroy-Cancellieri and V. Cerdà, *Trends Anal. Chem.*, 2016, **80**, 655–667.
- 15 B.-L. Su, X.-C. Ma, F. Xu, L.-H. Chen, Z.-Y. Fu, N. Moniotte, S. B. Maamar, R. Lamartine and F. Vocanson, *J. Colloid Interface Sci.*, 2011, **360**, 86–92.
- 16 F. Aydin, R. Çakmak, A. Levent and M. Soylak, *Appl. Organomet. Chem.*, 2020, **34**, e5481.
- 17 Y. Uppa, T. Taweeatanavanich, C. Kaewtong and N. Niamsa, *Environ. Technol.*, 2021, **42**, 1252–1259.
- 18 H. Ahmad and C. Liu, *J. Hazard. Mater.*, 2021, **415**, 125661.
- 19 M. Babaei, P. A. Azar, M. S. Tehrani, M. Farjaminezhad and S. W. Hussain, *J. Nanostruct. Chem.*, 2022, **12**, 249–261.
- 20 Y. Sun, Y. Gu and Q. Zha, *Chemosphere*, 2021, **280**, 130611.
- 21 S. Jakavula, N. R. Biata, K. M. Dimpe, V. E. Pakade and P. N. Nomngongo, *J. Hazard. Mater.*, 2021, **416**, 126175.
- 22 M. Hemmati, M. Rajabi and A. Asghari, *Microchim. Acta*, 2018, **185**, 160.
- 23 A. Stafiej and K. Pyrzynska, *Microchem. J.*, 2008, **89**, 29–33.
- 24 A. A. Gouda and S. M. Al Ghannam, *Food Chem.*, 2016, **202**, 409–416.
- 25 A. Rohanifar, L. B. Rodriguez, A. M. Devasurendra, N. Alipourasiabi, J. L. Anderson and J. R. Kirchoff, *Talanta*, 2018, **188**, 570–577.
- 26 T. Wang, Y. Chen, J. Ma, Z. Jin, M. Chai, X. Xiao, L. Zhang and Y. Zhang, *Talanta*, 2018, **180**, 254–259.
- 27 F. Bucatariu, C.-A. Ghiorghita, M.-M. Zaharia, S. Schwarz, F. Simon and M. Mihai, *ACS Appl. Mater. Interfaces*, 2020, **12**, 37585–37596.
- 28 L. Huang, W. Huang, R. Shen and Q. Shuai, *Food Chem.*, 2020, **330**, 127212.
- 29 M. Feng, P. Zhang, H.-C. Zhou and V. K. Sharma, *Chemosphere*, 2018, **209**, 783–800.
- 30 X. Li, W. Ma, H. Li, Q. Zhang and H. Liu, *Coord. Chem. Rev.*, 2020, **408**, 213191.
- 31 N. Fontanals, F. Borrull and R. M. Marcé, *Trends Anal. Chem.*, 2012, **41**, 15–26.
- 32 H. Niedermeyer, J. P. Hallett, I. J. Villar-Garcia, P. A. Hunt and T. Welton, *Chem. Soc. Rev.*, 2012, **41**, 7780–7802.
- 33 T. D. Ho, A. J. Canestraro and J. L. Anderson, *Anal. Chim. Acta*, 2011, **695**, 18–43.
- 34 M. Llaver, M. N. Oviedo, E. F. Fiorentini, P. Y. Quintas and R. G. Wuilloud, *Trends Environ. Anal. Chem.*, 2021, **31**, e00131.
- 35 M. Khraisheh, F. AlMamani, M. Inamdar, M. K. Hassan and M. A. Al-Ghouti, *J. Mol. Liq.*, 2021, **337**, 116421.
- 36 J. Nawala, B. Dawidziuk, D. Dziedzic, D. Gordon and S. Popiel, *TrAC, Trends Anal. Chem.*, 2018, **105**, 18–36.
- 37 M. Sajid, M. K. Nazal and I. Ihsanullah, *Anal. Chim. Acta*, 2021, **1141**, 246–262.
- 38 L. Vidal, M.-L. Riekkola and A. Canals, *Anal. Chim. Acta*, 2012, **715**, 19–41.
- 39 S. Platzer, M. Kar, R. Leyma, S. Chib, A. Roller, F. Jirsa, R. Krachler, D. R. MacFarlane, W. Kandioller and B. K. Keppler, *J. Hazard. Mater.*, 2017, **324**, 241–249.
- 40 L. Zhu, L. Guo, Z. Zhang, J. Chen and S. Zhang, *Sci. China: Chem.*, 2012, **55**, 1479–1487.



- 41 M. Gharehbaghi and F. Shemirani, *Anal. Methods*, 2012, **4**, 2879.
- 42 M. Ghaedi, D. Elhamifar, G. Negintaji and M. H. Banakar, *Int. J. Environ. Anal. Chem.*, 2013, **93**, 1525–1536.
- 43 S. Sadeghi and A. Z. Moghaddam, *Anal. Methods*, 2014, **6**, 4867.
- 44 H. M. Marwani, *J. Dispersion Sci. Technol.*, 2013, **34**, 117–124.
- 45 F. Adam, H. Osman and K. M. Hello, *J. Colloid Interface Sci.*, 2009, **331**, 143–147.
- 46 A. S. Amarasekara and O. S. Owereh, *Catal. Commun.*, 2010, **11**, 1072–1075.
- 47 D. A. Kotadia and S. S. Soni, *J. Mol. Catal. A: Chem.*, 2012, **353–354**, 44–49.
- 48 J. Li and H. Grennberg, *Chem. - Eur. J.*, 2006, **12**, 3869–3875.
- 49 J. Gao, G. Hu, J. Kang and G. Bai, *Talanta*, 1993, **40**, 195–200.
- 50 H. R. Fouladian and M. Behbahani, *Food Anal. Methods*, 2014, **8**, 982–993.
- 51 Z. A. Alothman, E. Yilmaz, M. Habila and M. Soylak, *Ecotoxicol. Environ. Saf.*, 2015, **112**, 74–79.
- 52 M. Khan, E. Yilmaz and M. Soylak, *J. Mol. Liq.*, 2016, **224**, 639–647.
- 53 O. Ozalp and M. Soylak, *Iran. J. Sci. Technol. Trans. A: Sci.*, 2021, **45**, 1971–1980.
- 54 N. Pourreza, R. Mirzajani, A. Reza Kiasat and R. Abdollahzadeh, *Quim. Nova*, 2012, **35**, 1945–1949.
- 55 M. Ghaedi, F. Ahmadi and M. Soylak, *J. Hazard. Mater.*, 2007, **147**, 226–231.
- 56 S. Tokalioglu, H. Büyükbas and S. Kartal, *J. Braz. Chem. Soc.*, 2006, **17**, 98–106.
- 57 C. E. Dogan and G. Akcin, *Anal. Lett.*, 2007, **40**, 2524–2543.
- 58 G. Venkatesh, A. K. Singh and B. Venkataramani, *Microchim. Acta*, 2004, **144**, 233–241.
- 59 C. Duran, A. Gundogdu, V. N. Bulut, M. Soylak, L. Elci, H. B. Sentürk and M. Tüfekci, *J. Hazard. Mater.*, 2007, **146**, 347–355.

